Check for updates

New Phytologist

Research

*Rapid report*

# *Arabidopsis thaliana* CYCLIC NUCLEOTIDE-GATED CHANNEL2 mediates extracellular ATP signal transduction in root epidermis

Author for correspondence:
*Julia Davies*
*Email: jmd32@cam.ac.uk*

Received: *27 August 2021*
Accepted: *16 January 2022*

**Limin Wang[1], Youzheng Ning[1], Jian Sun[1,2], Katie A. Wilkins[1], Elsa Matthus[1], Rose E. McNelly[1], Adeeba Dark[1], Lourdes Rubio[3], Wolfgang Moeder[4], Keiko Yoshioka[4], Anne-Aliénor Véry[5], Gary Stacey[6], Nathalie Leblanc-Fournier[7], Valérie Legué[7], Bruno Moulia[7] and Julia M. Davies[1]**

[1]Department of Plant Sciences, University of Cambridge, Cambridge, CB2 3EA, UK; [2]Institute of Integrative Plant Biology, School of Life Science, Jiangsu Normal University, Xuzhou 221116, China; [3]Facultad de Ciencias, Departamento de Botánica y Fisiología Vegetal, Universidad de Málaga, Málaga 29071, Spain; [4]Department of Cell & Systems Biology, University of Toronto, Toronto, ON M5S 3B2, Canada; [5]Biochimie & Physiologie Moléculaire des Plantes, UMR Université Montpellier, CNRS, INRAE, Institut Agro, Montpellier 34060, France; [6]Divisions of Plant Science and Technology, University of Missouri, Columbia, MO 65211, USA; [7]Université Clermont Auvergne, INRA, PIAF, Clermont-Ferrand F-63000, France

*New Phytologist* (2022)
**doi**: 10.1111/nph.17987

**Key words:** *Arabidopsis*, calcium, CNGC4, CYCLIC NUCLEOTIDE-GATED CHANNEL2 (CNGC2), depolarization, extracellular ATP, plasma membrane potential, root epidermis.

## Summary

- Damage can be signalled by extracellular ATP (eATP) using plasma membrane (PM) receptors to effect cytosolic free calcium ion ($[Ca^{2+}]_{cyt}$) increase as a second messenger. The downstream PM $Ca^{2+}$ channels remain enigmatic. Here, the *Arabidopsis thaliana* $Ca^{2+}$ channel subunit CYCLIC NUCLEOTIDE-GATED CHANNEL2 (CNGC2) was identified as a critical component linking eATP receptors to downstream $[Ca^{2+}]_{cyt}$ signalling in roots.
- Extracellular ATP-induced changes in single epidermal cell PM voltage and conductance were measured electrophysiologically, changes in root $[Ca^{2+}]_{cyt}$ were measured with aequorin, and root transcriptional changes were determined by quantitative real-time PCR. Two *cngc2* loss-of-function mutants were used: *cngc2-3* and *defence not death1* (which expresses cytosolic aequorin).
- Extracellular ATP-induced transient depolarization of Arabidopsis root elongation zone epidermal PM voltage was $Ca^{2+}$ dependent, requiring CNGC2 but not CNGC4 (its channel co-subunit in immunity signalling). Activation of PM $Ca^{2+}$ influx currents also required CNGC2. The eATP-induced $[Ca^{2+}]_{cyt}$ increase and transcriptional response in *cngc2* roots were significantly impaired.
- CYCLIC NUCLEOTIDE-GATED CHANNEL2 is required for eATP-induced epidermal $Ca^{2+}$ influx, causing depolarization leading to $[Ca^{2+}]_{cyt}$ increase and damage-related transcriptional response.

## Introduction

Extracellular ATP (eATP) has been shown to contribute to plant growth and development, stress responses, immunity, and damage (Matthus *et al.*, 2019a). Two plasma membrane (PM) coreceptors for eATP, DOES NOT RESPOND TO NUCLEOTIDES1 (P2K1/DORN1) and P2K2, have been identified recently in *Arabidopsis thaliana*, with P2K1/DORN1 transphosphorylating P2K2 (Choi *et al.*, 2014; Pham *et al.*, 2020). P2K1/DORN1 commands an eATP-dependent transient increase of cytosolic free calcium ions ($[Ca^{2+}]_{cyt}$) as a second messenger (Choi *et al.*, 2014). The root $[Ca^{2+}]_{cyt}$ response to eATP (the 'signature') has a greater reliance on $Ca^{2+}$ influx across the PM than the release of $Ca^{2+}$ from intracellular stores (Demidchik *et al.*, 2009; Rincón-Zachary *et al.*, 2010). Lowering external $Ca^{2+}$ from 10 to 0.1 mM causes an 85% decrease in the $[Ca^{2+}]_{cyt}$ response (Demidchik *et al.*, 2003). $Ca^{2+}$

© 2022 The Authors
*New Phytologist* © 2022 New Phytologist Foundation
This is an open access article under the terms of the Creative Commons Attribution License, which permits use, distribution and reproduction in any medium, provided the original work is properly cited.

influx across the PM helps explain the depolarizing effect that eATP has on root PM voltage (Lew & Dearnaley, 2000; Dindas *et al.*, 2018), especially given that eATP causes instantaneous $[Ca^{2+}]_{cyt}$ increase and a cytosolic acidification consistent with PM $H^+$-ATPase inhibition in Arabidopsis roots (Waadt *et al.*, 2020). Indeed, patch clamp electrophysiology has revealed eATP and P2K1/DORN1-dependent $Ca^{2+}$-permeable channel conductances in Arabidopsis root epidermal PM (Demidchik *et al.*, 2009; Wang *et al.*, 2018, 2019) that could contribute to PM depolarization and $[Ca^{2+}]_{cyt}$ increase. However, the identity of the channels remains unknown. Here, data support the involvement of a CYCLIC NUCLEOTIDE-GATED CHANNEL (CNGC).

Arabidopsis has a family of 20 CNGC subunits, with members contributing to $[Ca^{2+}]_{cyt}$ signatures evoked by abiotic stress, pathogen attack, and hormones (Jarratt-Barnham *et al.*, 2021). Because eATP accumulates during pathogen infection and acts as a damage-associated molecular pattern (DAMP) that drives a transcriptional response through P2K1/DORN1 (Choi *et al.*, 2014; Jewell *et al.*, 2019; Kumar *et al.*, 2020), CNGCs involved in pathogen sensing could also be acting in the eATP pathway. CYCLIC NUCLEOTIDE-GATED CHANNEL2 is a key candidate for testing, as it operates in root signalling (Chakraborty *et al.*, 2021), it is involved in both DAMP and pathogen-associated molecular pattern (PAMP) signalling, and it generates a PM hyperpolarization-activated $Ca^{2+}$-permeable channel conductance (Qi *et al.*, 2010; Tian *et al.*, 2019). Cyclic Nucleotide-Gated Channel2's closest paralogue, CNGC4, can interact with CNGC2, and these two subunits are hypothesized to form a heteromeric channel in PAMP signalling (Chin *et al.*, 2013; Tian *et al.*, 2019). Cyclic Nucleotide-Gated Channel2 and CNGC4 could potentially work together in the eATP pathway.

Here, two Arabidopsis *cngc2* loss of function mutants were used: *cngc2-3* and *defence not death1* (*dnd1*; which expresses cytosolic aequorin). Extracellular ATP-induced depolarization of PM voltage has been used as a diagnostic of PM $Ca^{2+}$ channel activity in single epidermal and cortical root cells. Results show an absolute requirement for CNGC2 but not CNGC4 in the epidermis. Patch clamp electrophysiological analysis of eATP-induced PM $Ca^{2+}$ influx conductance of epidermal cells confirmed an absolute requirement for CNGC2. Both root eATP-induced $[Ca^{2+}]_{cyt}$ signature and transcriptional response were impaired by loss of CNGC2 function.

## Materials and Methods

### Plant material

Arabidopsis lines were in the Columbia (Col-0) ecotype. *dorn1-1*, *dorn1-3*, *p2k2*, and *p2k1p2k2* mutants were as described previously (Choi *et al.*, 2014; Pham *et al.*, 2020). *cngc2-3* (transfer DNA (T-DNA) insertion line Salk-066908) was described previously by Chin *et al.*, 2013. Complemented *cngc2-3* was generated with the CNGC2 coding sequence under the control of its endogenous promoter (Supporting Information Methods S1). *dnd1 cngc2* loss-of-function mutant constitutively expressing cytosolic (apo)aequorin was described by Qi *et al.*, 2010. *cngc4-5* (SALK_081369; Tian *et al.*, 2019) was obtained from the Nottingham Arabidopsis Stock Centre. Genotyping of insertional and complemented mutants is described in Methods S1. Primers are listed in Table S1. Growth conditions are described in Methods S2. Plants at 7–14 d old were used unless stated otherwise.

### Membrane potential measurements

Plasma membrane potential $E_m$ of root elongation zone cells was measured using a glass microelectrode. A plant was fixed in a plexiglass chamber and immersed in assay solution (10 ml) containing 2 mM calcium chloride ($CaCl_2$; with or without 5 mM ethylene glycol-bis(β-aminoethyl ether)-*N*,*N*,*N*′,*N*′-tetraacetic acid) (EGTA) or with or without 0.5 mM lanthanum chloride ($LaCl_3$)), 0.1 mM potassium chloride (KCl), 1 mM MES–Tris (pH 6.0) for at least 30 min before impalement. Microelectrode construction, recording circuitry, and impalement are described in Methods S3. After observing a stable $E_m$ (> 6 min), eATP (ATP magnesium salt (MgATP) or ATP disodium salt ($Na_2ATP$); Sigma) was added to the chamber (final concentration 300 µM in the assay medium, pH 6.0). In controls, magnesium sulphate ($MgSO_4$) or sodium sulphate ($Na_2SO_4$) was added.

### Patch clamp recordings

Protoplasts were isolated from root elongation zone epidermis, with origin confirmed using the N9093 epidermal-specific green fluorescent protein reporter line as described by Wang *et al.* (2019). Details of isolation, patch clamp solutions, and protocols are in Methods S4.

### Cytosolic free calcium ion measurement

Excised primary roots of Col-0 and *dnd1* expressing cytosolic (apo) aequorin were used for luminescence-based quantification of $[Ca^{2+}]_{cyt}$. Roots were placed individually into a 96-well plate (one root per well) and incubated overnight at room temperature in darkness with 10 µM coelenterazine in 100 µl of buffer: 2 mM $CaCl_2$, 0.1 mM KCl, 1 mM MES–Tris (pH 5.6). $CaCl_2$ was included to maintain a similar level to that of the growth medium. Samples were washed with coelenterazine-free buffer and left to recover for at least 20 min in darkness. A FLUOstar Optima plate reader (BMG Labtech, Ortenberg, Germany) was used to record luminescence as described in Matthus *et al.* (2019b). $[Ca^{2+}]_{cyt}$ was calculated as described by Knight *et al.*, 1997.

### Analysis of gene expression

Total RNA was extracted from roots (frozen in liquid nitrogen) using the RNAeasy Plant Mini Kit (Qiagen) and subjected to DNase I treatment (RNAse-free DNAse kit; Qiagen). Complementary DNA (cDNA) was synthesized using the QuantiTect Reverse Transcription Kit (Qiagen). Quantitative real-time (qRT)-PCR was performed in a Rotor-Gene 3000 thermocycler with the Rotor-Gene™ SYBR® Green PCR Kit (Qiagen). *UBQ10* and


© 2022 The Authors
*New Phytologist* © 2022 New Phytologist Foundation

*TUB4* acted as internal controls. Primers are listed in Table S1. Further details are in Methods S5.

### Statistical analysis

Data normality was first analysed with the Shapiro–Wilk test in R. Student's *t*-test or Tukey's honestly significant difference was used for parametric data comparison, whereas the Mann–Whitney *U* test was used to compare the nonparametric data.

## Results

### AtCNGC2 mediates the extracellular-ATP-induced depolarization of root epidermal plasma membrane voltage and does not require AtCNGC4

The stable resting membrane voltage $E_m$ of a single Col-0 root elongation zone epidermal cell (Fig. 1a) was significantly but transiently depolarized by 300 μM eATP (Fig. 1b). This concentration of eATP was found previously to activate a PM $Ca^{2+}$ influx conductance in this cell type (Wang *et al.*, 2019). Mean maximal depolarization from $-118.9 \pm 4.8$ to $-69.2 \pm 7.6$ mV (Fig. 1c,d; Table S2) occurred $1.8 \pm 0.3$ min after eATP application (MgATP or $Na_2ATP$), and $E_m$ recovered fully after $14.7 \pm 2.2$ min (Fig. 1e,f) in the continued presence of eATP. In controls, neither 300 μM $MgSO_4$ nor 300 μM $Na_2SO_4$ (Figs 1g,h, S1a,b) affected $E_m$, confirming that the response was due to eATP. Incubation with 5 mM EGTA (to chelate extracellular $Ca^{2+}$) abolished the response to 300 μM eATP (Figs 1g,h, S1c), showing that depolarization required $Ca^{2+}$ influx. However, as EGTA treatment resulted in a less negative $E_m$ that could have compromised depolarization, a further test of $Ca^{2+}$ influx was conducted. Addition of 0.1 mM $LaCl_3$ as a blocker of PM $Ca^{2+}$-permeable channels prevented significant depolarization by eATP (Figs 1g,h, S1d). The loss-of-function *cngc2-3* mutant (T-DNA insert in second exon) and the complemented *cngc2-3,CNGC2::CNGC2* mutant (Fig. S2a–c) were then analysed. Expression levels of *P2K1/DORN1* and the coreceptor *P2K2* were normal in *cngc2-3* roots, indicating that eATP perception itself would be unimpaired (Fig. S2d). There were no significant differences in resting $E_m$ between genotypes (Table S2). In contrast to Col-0, 300 μM eATP failed to depolarize *cngc2-3* $E_m$ (Fig. 1b–d; Table S2). Complementation fully restored the mutant's $E_m$ response to eATP (depolarization and recovery time) (Fig. 1b–e), but maximum $E_m$ depolarization occurred sooner than in Col-0 (Fig. 1f). This may reflect the approximately doubled abundance of *CNGC2* transcript in the complemented mutant, although this was not statistically significant (Fig. S2e). To verify the *cngc2-3* results, the *CNGC2 dnd1* mutant (Fig. S3a–c) was also tested. This has a single point mutation causing a stop codon in the third exon and expresses cytosolic aequorin (Qi *et al.*, 2010). Resting *dnd1* $E_m$ was not significantly different to those of other genotypes and was unaffected by eATP treatment (Fig. S3d–f; Table S2). These results show that the eATP-induced and $Ca^{2+}$-dependent PM $E_m$ response is reliant on CNGC2.

Elongation zone epidermal cells of the *dorn1-3* loss-of-function mutant, the *dorn1-1* kinase mutant, and the *p2k2* mutant all retained a small but significant depolarization of $E_m$ when challenged with 300 μM eATP (Fig. S4a–d; Table S2). *CNGC2* transcript levels were normal in both *dorn1-3* and *p2k2* mutant roots, so their lowered response is most likely due to loss of receptor function rather than channel function (Fig. S4e). The *dorn1-3p2k2* double mutant (*p2k1p2k2*) also sustained a small but significant depolarization of $E_m$ when challenged with 300 μM eATP, but this was not significantly different to that caused by the $Na_2SO_4$ control (Fig. S5a–c; Table S2; $P = 0.74$). Under control conditions, the *p2k1p2k2* mutant had a significantly more negative $E_m$ ($-143.9 \pm 4.3$ mV; $n = 10$) than its paired Col-0 wild-type ($-129.9 \pm 4.6$ ($n = 5$); $P = 0.005$), and this may help explain why sodium ions ($Na^+$) caused a depolarization in this mutant but not in Col-0. Overall, the results suggest that the two receptors working together are sufficient to initiate the eATP-induced depolarization of $E_m$ and that CNGC2 is an absolute requirement in this cell type.

Cyclic Nucleotide-Gated Channel2 has been shown to interact with CNGC4 in immune signalling (Chin *et al.*, 2013; Tian *et al.*, 2019). Here, the root elongation zone epidermis of the *cngc4*-5 loss-of-function mutant (Fig. S6a–d) was impaled and tested with 300 μM eATP. The eATP caused a significant depolarization of $E_m$ to $-69.4 \pm 10.9$ mV, similar to Col-0 wild-type ($P > 0.05$; Fig. S6e–g; Table S2). These results show that CNGC2 controls the PM $E_m$ response to eATP without the need for CNGC4.

### Plasma membrane calcium-ion currents induced by extracellular ATP in Col-0 root epidermal protoplasts require CNGC2

Whole-cell currents across the PM of root elongation zone epidermal protoplasts Wang *et al.* (2019) of Col-0 and *cngc2-3* were recorded. No significant differences in control currents or reversal potential were found between genotypes (mean ± SE reversal potential: Col-0 $-59 \pm 16.3$ mV, $n = 4$; *cngc2-3* $-35 \pm 8.9$, $n = 4$). For Col-0, 300 μM eATP activated whole-cell inward current upon membrane hyperpolarization, but not outward current upon membrane depolarization (Fig. 2a). No effect of $Na^+$ as the salt control was found in previous trials (Wang *et al.*, 2018, 2019). Analysis of the reversal potential of eATP-activated currents (average control (no ATP) currents were subtracted from average eATP-activated currents (Wang *et al.*, 2013)) revealed an approximate value of +22 mV ($n = 4$), far from the equilibrium potentials of potassium ions ($K^+$; −79 mV) and chloride ions (−28 mV) and indicating $Ca^{2+}$ permeability. Extracellular ATP-activated inward current was significantly inhibited by 100 μM gadolinium ions ($Gd^{3+}$), a plant $Ca^{2+}$ channel blocker that is effective against CNGC2 (Demidchik *et al.*, 2009; Wang *et al.*, 2018, 2019; Tian *et al.*, 2019; Fig. 2a). These results suggest that $Ca^{2+}$ influx across the PM contributed to the eATP-activated current in Col-0. As $Gd^{3+}$ is an effective blocker of a variety of PM $Ca^{2+}$-permeable channels (Demidchik *et al.*, 2002, 2009; Wang *et al.*, 2018, 2019) it is likely that it also blocked $Ca^{2+}$-permeable channels that were *not* activated by eATP, causing the significant reduction in inward current in the presence of both eATP and $Gd^{3+}$ to below the control value. The eATP-activated $Ca^{2+}$ inward current was absent from *dorn1-3* PM (Fig. S7). At resting $E_m$ of

© 2022 The Authors
*New Phytologist* © 2022 New Phytologist Foundation

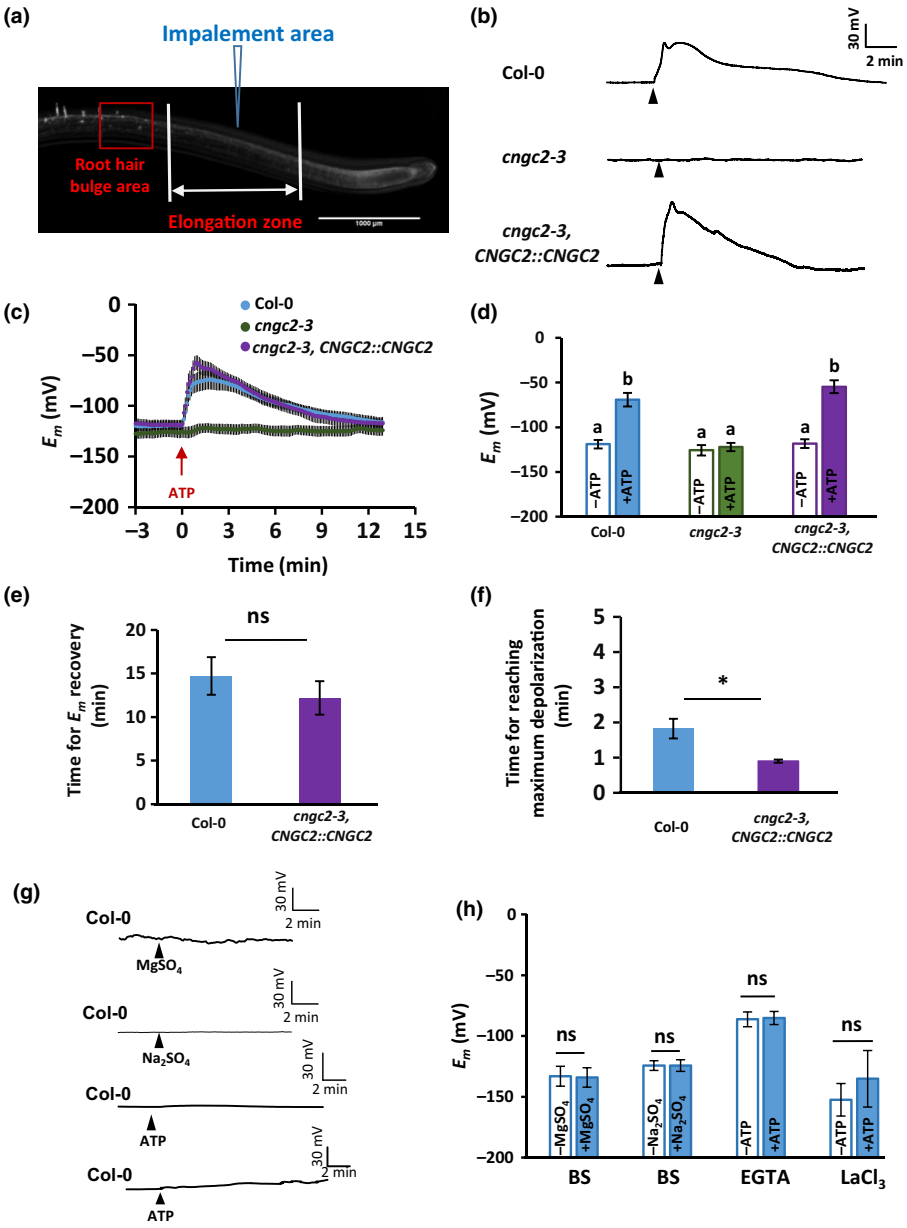


**Fig. 1** CYCLIC NUCLEOTIDE-GATED CHANNEL2 (CNGC2) is required for extracellular ATP (eATP)-induced depolarization of primary root elongation zone epidermal plasma membrane potential $E_m$. (a) A representative example of an *Arabidopsis* Col-0 root indicating the elongation zone where a single epidermal or cortical cell was impaled with a microelectrode (represented by the blue triangle). Bar, 0.1 cm. (b) Representative epidermal $E_m$ recordings from Col-0, *cngc2-3*, and *cngc2-3,CNGC2::CNGC2* treated with 300 μM eATP (black triangles indicate addition). (c) Mean ± SE time courses of the response to 300 μM eATP for Col-0 ($n = 9$), *cngc2-3* ($n = 9$), and *cngc2-3,CNGC2::CNGC2* ($n = 5$). The chemical addition time was set to zero on the *x*-axis. (d) Comparison of mean ± SE $E_m$ before eATP (−ATP) and after eATP treatment (+ATP; maximum depolarization). Different lower-case letters on the top of vertical bars indicate significant difference between means ($P < 0.05$). (e) Col-0 and *cngc2-3,CNGC2::CNGC2* took similar times for $E_m$ to recover from depolarization. (f) *cngc2-3,CNGC2::CNGC2* $E_m$ depolarized more rapidly than Col-0 in response to eATP. (g) Representative epidermal $E_m$ recordings from Col-0. Top trace: response to 300 μM magnesium sulphate ($MgSO_4$; $n = 8$); second trace: response to 300 μM sodium sulphate ($Na_2SO_4$; $n = 6$); third trace: response to 300 μM eATP in the presence of 5 mM ethylene glycol-bis(β-aminoethyl ether)-*N*,*N*,*N*′,*N*′-tetraacetic acid) (EGTA; $n = 5$); bottom trace: response to 300 μM eATP in the presence of 0.5 mM lanthanum chloride ($LaCl_3$; $n = 3$). Mean time courses are in Supporting Information Fig. S1. (h) Comparison of mean ± SE $E_m$ before and after addition of 300 μM $MgSO_4$ or $Na_2SO_4$ to bath solution (BS) and before and after addition of eATP in the presence of 5 mM EGTA or 0.5 mM $LaCl_3$ in the BS. Bath solution contained 2 mM calcium chloride, 0.1 mM potassium chloride, 1 mM MES–Tris (pH 6.0). *, $P < 0.05$; ns, not significant.

Col-0 epidermal cells (*c.* −120 mV) the eATP-activated current would deliver $Ca^{2+}$ to the cytosol, which would both elevate $[Ca^{2+}]_{cyt}$ and initiate depolarization. It can be inferred that some eATP-activated $Ca^{2+}$ influx should have occurred in membrane voltage trials at the less negative $E_m$ caused by EGTA (−85.2 ± −5.4 mV; Figs 1(g,h), S1c) but this was not observed, further supporting the role of $Ca^{2+}$ influx in eATP-induced depolarization of $E_m$. In contrast to Col-0, PM whole-cell currents of *cngc2-3*


© 2022 The Authors
*New Phytologist* © 2022 New Phytologist Foundation

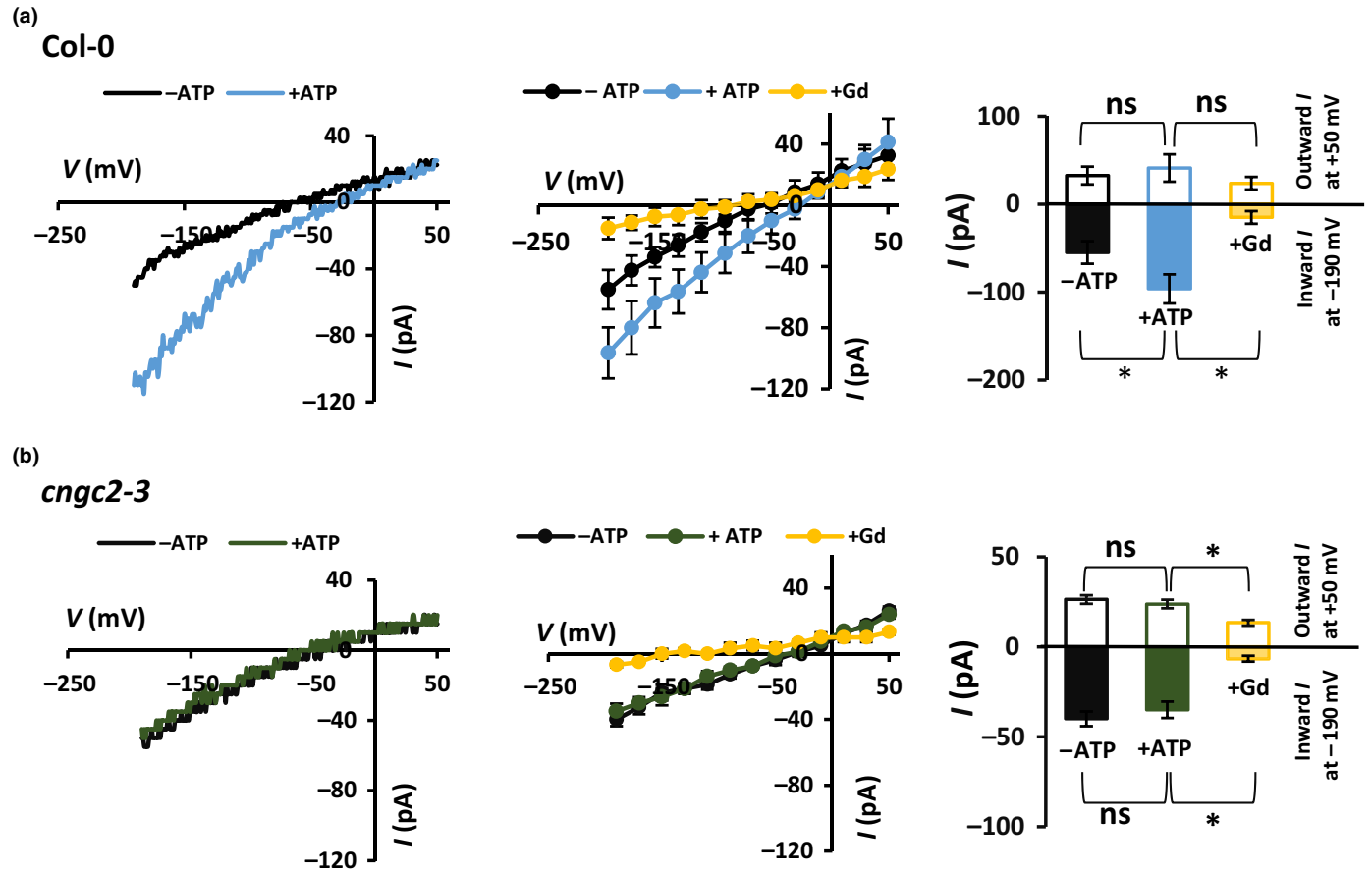


**Fig. 2** Extracellular ATP (eATP) activates inward currents in *Arabidopsis* Col-0 but not *cngc2-3* root elongation zone epidermal protoplasts. (a) Left panel: typical whole-cell plasma membrane currents in Col-0 protoplasts before (−; black) and after (+; light blue) application of 300 μM eATP. Extracellular ATP effects were observed 30 s to 3 min after addition. Bath solution contained 50 mM calcium chloride, 1 mM potassium chloride (KCl), and 10 mM MES–Tris (pH 5.6). Pipette solution comprised 5 mM barium chloride, 20 mM KCl, and 10 mM HEPES–Tris (pH 7.5). Centre panel: mean ± SE current-voltage (*I–V*) relationships of Col-0 before (−), after (+) ATP and in 100 μM gadolinium ions ($Gd^{3+}$; dark blue; the calcium channel blocker was applied after eATP treatment) ($n = 4$). Right panel: comparison of the inward currents at −190 mV (solid bars) and the outward currents at +50 mV (hollow bars) before and after eATP addition and in the presence of $Gd^{3+}$. $Gd^{3+}$ block of control inward currents is also evident. (b) As (a), but for *cngc2-3* protoplasts. The mutant did not respond to eATP even with an extended observation period (10 min). Data are means ± SE ($n = 4$; *, $P < 0.05$; ns, not significant).

(either inward or outward) failed to respond to 300 μM eATP (Fig. 2b). $Gd^{3+}$ (100 μM) blocked inward and outward currents in the presence of eATP, but these currents were not investigated further (Fig. 2b). Thus, the results strongly suggest that the eATP-activated inward current in Col-0 would be due to the hyperpolarization-activated $Ca^{2+}$ influx through CNGC2, helping to explain how eATP failed to depolarize the $E_m$ of the *cngc2* mutants.

## Extracellular-ATP-induced cytosolic free calcium ion increase in roots is impaired in *dnd1*

The requirement for CNGC2 in eATP-activated epidermal PM depolarization and $Ca^{2+}$ influx conductance should manifest in impaired eATP-induced $[Ca^{2+}]_{cyt}$ elevation in the *dnd1* mutant, which expresses cytosolic (apo)aequorin as a bioluminescent $[Ca^{2+}]_{cyt}$ reporter. The typical monophasic $[Ca^{2+}]_{cyt}$ increase ('touch response') after sodium chloride (NaCl) addition (control for mechanostimulation and cation effect of $Na_2ATP$) was observed in individual roots of Col-0 and *dnd1*. The amplitude of the touch peak and total $[Ca^{2+}]_{cyt}$ mobilized did not differ significantly between genotypes (Fig. 3a). By contrast, 300 μM eATP caused a biphasic $[Ca^{2+}]_{cyt}$ increase (after the touch response) in both Col-0 and *dnd1* roots (Fig. 3b), confirming that this part of the $[Ca^{2+}]_{cyt}$ signature was caused by eATP. This biphasic signature ('peak 1' and 'peak 2') was observed in previous studies on Arabidopsis roots and seedlings using aequorin (Demidchik *et al.*, 2003; Tanaka *et al.*, 2010; Matthus *et al.*, 2019a,b; Mohammad-Sidik *et al.*, 2021) and also root tips using YC3.6 (Tanaka *et al.*, 2010). *dnd1* roots were significantly impaired in the amplitude of both of the eATP-induced $[Ca^{2+}]_{cyt}$ peaks and also total $[Ca^{2+}]_{cyt}$ mobilized (Fig. 3d). Significant impairment was also observed at 100 μM and 1 mM eATP (Fig. S8). Since P2K1/DORN1 governs the eATP-induced $[Ca^{2+}]_{cyt}$ signature in Arabidopsis roots (Matthus *et al.*, 2019a), impairment of the $[Ca^{2+}]_{cyt}$ response in *dnd1* helps place CNGC2 downstream of that eATP receptor, consistent with the electrophysiological data presented here.

© 2022 The Authors
*New Phytologist* © 2022 New Phytologist Foundation

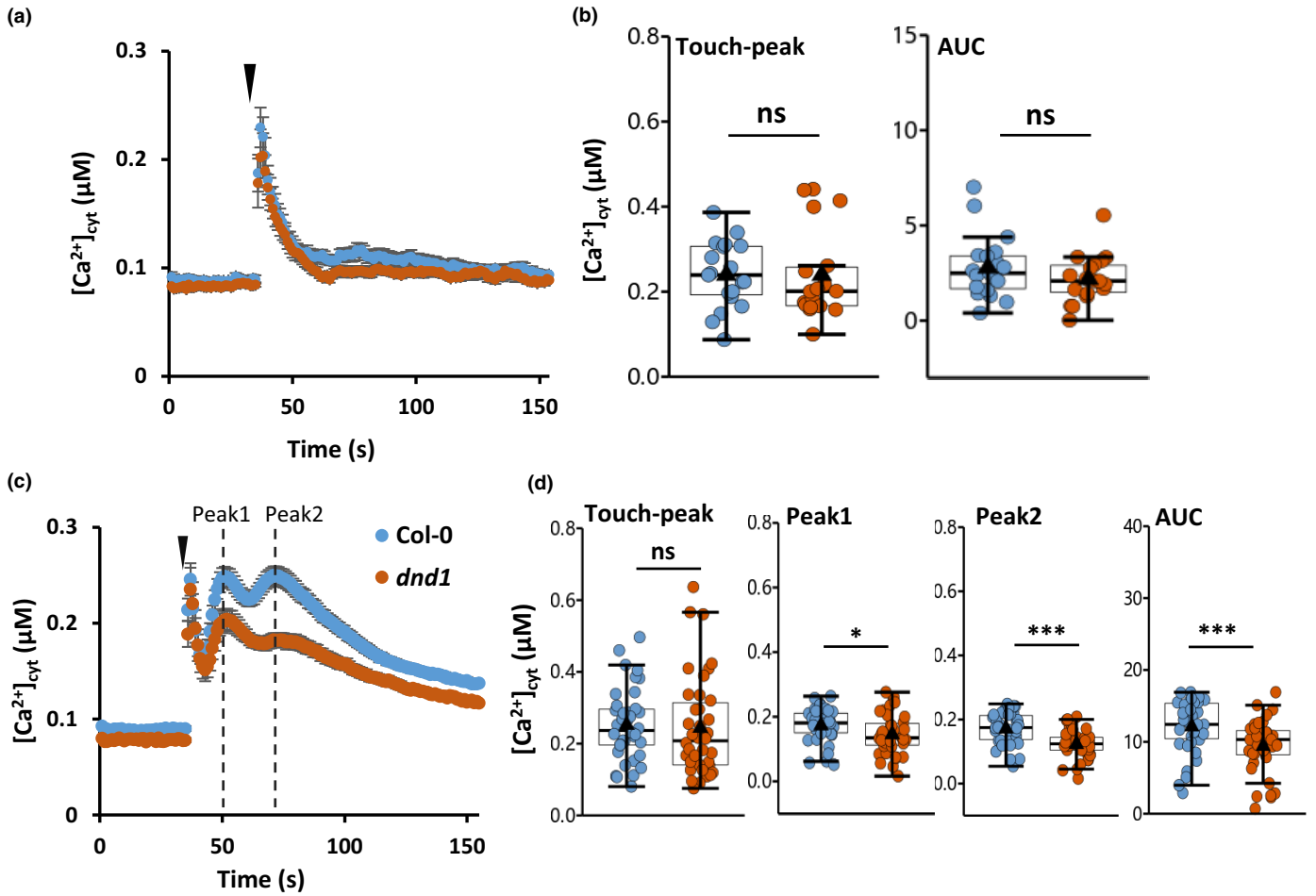


**Fig. 3** CYCLIC NUCLEOTIDE-GATED CHANNEL2 (CNGC2) contributes to the extracellular ATP (eATP)-induced cytosolic free calcium ion ($[Ca^{2+}]_{cyt}$) increase in Arabidopsis roots. (a) Mean ± SE $[Ca^{2+}]_{cyt}$ time-course in control experiments ($n$ = 18–19 roots in three independent trials). Sodium chloride was applied at 35 s to individual excised roots of Col-0 or *defence not death1* (*dnd1*) (black inverted triangle; 0.6 mM final concentration). Assay solution contained 2 mM $Ca^{2+}$ to match plasma membrane potential $E_m$ recordings. (b) Left panel: amplitude of touch-induced peak $[Ca^{2+}]_{cyt}$ increase after baseline subtraction. The *dnd1* response was not normally distributed, and the Mann–Whitney test was used in significance testing. Right panel: area under the curve (AUC) after baseline subtraction was analysed as an estimate of total $[Ca^{2+}]_{cyt}$ mobilized (Matthus *et al*., 2019b). (c) Mean ± SE $[Ca^{2+}]_{cyt}$ time-course with 300 μM eATP applied at 35 s ($n$ = 38 for both Col-0 and *dnd1* in three independent trials). Dotted lines indicate time of peak response of Col-0. (d) *dnd1* had a significantly smaller $[Ca^{2+}]_{cyt}$ response when compared with Col-0, but not in the touch peak. The *dnd1* response for the touch peak was not normally distributed, and the Mann–Whitney test was used in significance testing. Peaks were compared with Col-0 at the equivalent time point. Each dot in the box plots represents an individual recording. The middle line and the triangle in the box plot are the median and mean, respectively. The box outline (hinges) denotes median of the upper and the lower half of the data. The bars denote entirety of data excluding outliers; outliers are depicted by individual points outside the boxplot bars. *, $P < 0.05$; ***, $P < 0.001$; ns, not significant.

## Root cortical plasma membrane depolarization does not require CNGC2 but may require CNGC4

The residual eATP-induced $[Ca^{2+}]_{cyt}$ increase seen in *dnd1* roots suggests CNGC2-independent $Ca^{2+}$ influx pathways in other cells, such as the cortex. Cortical cells also increase $[Ca^{2+}]_{cyt}$ in response to eATP (Krogman *et al*., 2020). Cyclic Nucleotide-Gated Channel2 redundancy was investigated by measuring elongation zone cortical cell $E_m$. Resting Col-0 cortical cell $E_m$ was −131.6 ± 9.1 mV (Fig. S9a; Table S2), which was not significantly different to the epidermis. Application of eATP (300 μM) to the root transiently and significantly depolarized the cortical PM (Fig. S9a; Table S2). There was no significant difference between cortex and epidermis in terms of the maximum depolarization amplitude, the time to reach the maximum depolarization, or recovery time. The $E_m$ of elongation zone cortical cells in the two CNGC2 mutants was then investigated. Unlike the null response of epidermal cells of *cngc2-3* and *dnd1*, addition of eATP to the root triggered cortical $E_m$ depolarization in both mutants (Fig. S9b,c; Table S2). No significant difference in the PM $E_m$ before (no ATP added) or after ATP (ATP added) was observed between Col-0 and these two mutants (Fig. S9e), indicating that CNGC2 is not involved in this cell type. The *cngc4-5* mutant still supported a significant depolarization of cortical $E_m$ when eATP was added to the root (Fig. S9d,e; Table S2), but this was significantly smaller than that found previously in its epidermal cells (cortex, 21.6 ± 6.8 mV; epidermis, 62.2 ± 8.8 mV; $P$ = 0.012). This indicates a CNGC4-dependent pathway in the cortex. The residual


© 2022 The Authors
*New Phytologist* © 2022 New Phytologist Foundation

depolarization in the *cngc4-5* implies involvement of other CNGCs (but not CNGC2) or other transport systems (Fig. S9f). Together, the results help explain the residual eATP-induced $[Ca^{2+}]_{cyt}$ increase in *dnd1* roots; CNGC2 does not operate in all other cells.

## CNGC2 is implicated in extracellular-ATP-responsive gene expression

The eATP-responsive transcriptome is highly enriched in defence-related and wound-response genes, including *MITOGEN-ACTIVATED PROTEIN KINASE 3* (*MPK3*), *WRKY DNA-BINDING PROTEIN 40* (*WRKY40*), *CALCIUM-DEPENDENT PROTEIN KINASE 28* (*CPK28*), and the cysteine protease *METACASPASE 7* (*MC7*) (Choi *et al.*, 2014; Jewell *et al.*, 2019). Transcriptional upregulation of those genes by eATP is P2K1/DORN1 dependent (Choi *et al.*, 2014; Jewell *et al.*, 2019), and their response to eATP was examined here in Col-0, *cngc2-3*, and *cngc2-3,CNGC2::CNGC2* roots by qRT-PCR. Extracellular ATP (300 μM for 30 min) significantly upregulated expression of all four genes in Col-0, with no significant difference between Col-0 and *cngc2-3,CNGC2::CNGC2* (Fig. 4). However, transcript levels of *MPK3*, *WRKY40*, *CPK28*, and *MC7* were all significantly lower in *cngc2-3* compared with Col-0 or (with the exceptions of *CPK28* and *MC7*) compared with *cngc2-3,CNGC2::CNGC2*

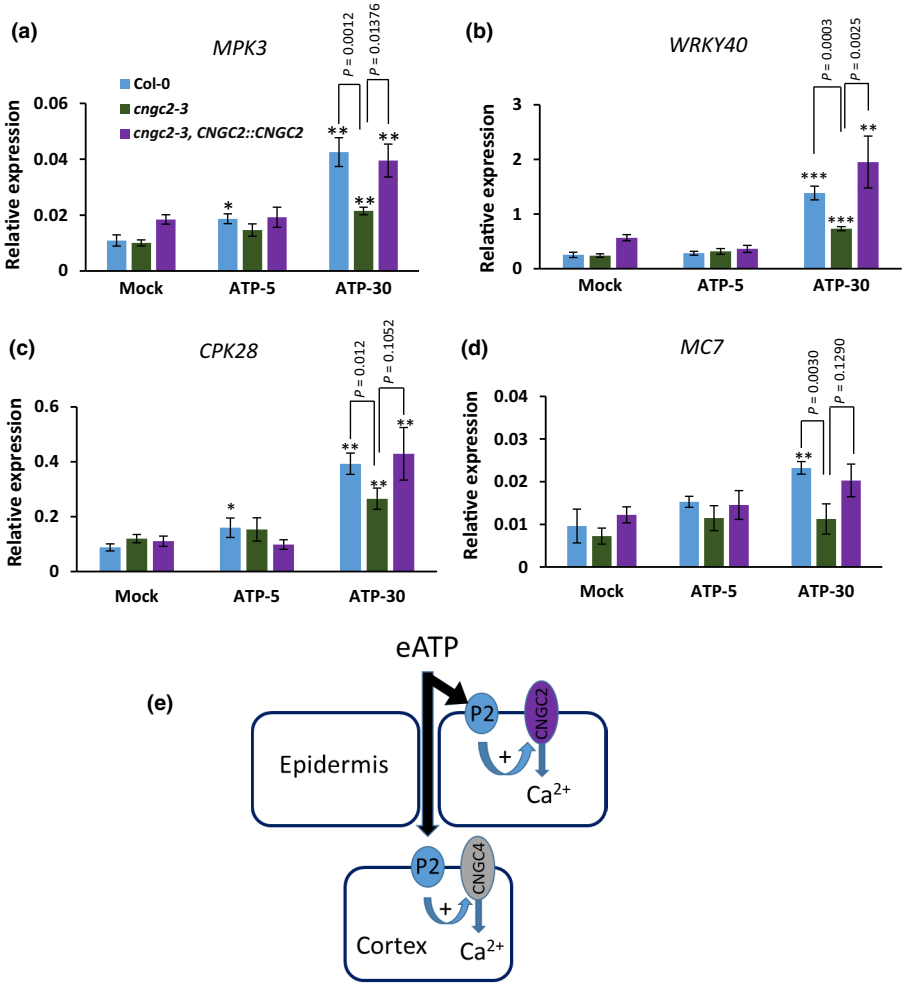


**Fig. 4** CYCLIC NUCLEOTIDE-GATED CHANNEL2 (CNGC2) is implicated in the extracellular ATP (eATP)-induced transcriptional response in Arabidopsis roots. Col-0, *cngc2-3*, and *cngc2-3,CNGC2::CNGC2* whole roots were treated with control (sodium chloride) buffer (Mock) or 300 μM eATP for 5 min (ATP-5) or 30 min (ATP-30). Two housekeeping genes, *AtUBQ10* and *AtTUB4*, were used for data normalization. Data are mean ± SE from three independent trials with $n > 4$ biological replicates. (a) Results for *MITOGEN-ACTIVATED PROTEIN KINASE 3* (*MPK3*). (b) Results for *WRKY DNA-BINDING PROTEIN 40* (*WRKY40*). (c) Results for *CALCIUM-DEPENDENT PROTEIN KINASE 28* (*CPK28*). (d) Results for *METACASPASE 7* (*MC7*). Significant differences between *cngc2-3* and the other two genotypes were found at ATP-30, and *P* values are shown. No significant differences were observed between Col-0 and *cngc2-3,CNGC2::CNGC2* at ATP-30. Asterisks indicate the statistical significance relative to the mock treatment (*, $P < 0.05$; **, $P < 0.01$; ***, $P < 0.001$). (e) Summary of possible signalling events at epidermis and cortex. DOES NOT RESPOND TO NUCLEOTIDES1 (DORN1/P2K1) and P2K2 (P2) together promote CNGC2 channel opening to mediate calcium ion ($Ca^{2+}$) influx, plasma membrane potential $E_m$ depolarization, and cytosolic free $Ca^{2+}$ ($[Ca^{2+}]_{cyt}$) increase. The mechanism is unknown, but it could include phosphorylation or direct production of cyclic nucleotide monophosphates by cryptic catalytic centres (Al-Younis *et al*., 2021). Extracellular ATP could follow the apoplastic pathway to initiate events in cortical cells, potentially through the P2 receptor complex and with CNGC4 as a component of $Ca^{2+}$ influx, $E_m$ depolarization and $[Ca^{2+}]_{cyt}$ increase. Other stimuli could be transmitted from the epidermis to the cortex in a CNGC2-independent pathway.

© 2022 The Authors
*New Phytologist* © 2022 New Phytologist Foundation

(Fig. 4). Thus, CNGC2 can be required for the eATP transcriptional response.

## Discussion

Effects of eATP on plants were reported almost half a century ago (Jaffe, 1973), yet relatively few components of eATP signalling pathways have been identified. A forward genetic screen based on eATP's ability to increase $[Ca^{2+}]_{cyt}$ led to the identification of the first angiosperm eATP receptor, P2K1/DORN1 (Choi *et al.*, 2014). Here, eATP's ability to depolarize root PM $E_m$ (Lew & Dearnaley, 2000) was used in a targeted gene approach. Depolarization can arise from $Ca^{2+}$ influx across the PM (Dindas *et al.*, 2018), and eATP causes a rapid $[Ca^{2+}]_{cyt}$ increase in roots that could initiate depolarization (Waadt *et al.*, 2020) as a multiconductance process (Wang *et al.*, 2019). Here, eATP-induced depolarization required extracellular $Ca^{2+}$ (Figs 1g,h, S1c,d), showing its reliance on $Ca^{2+}$ influx. Thus, the unresponsiveness of *cngc2* mutant root elongation zone epidermal PM to eATP (Fig. 1) is consistent with its lack of eATP-induced PM $Ca^{2+}$ influx currents (Fig. 2) and reveals CNGC2 as a necessary component for initiating depolarization downstream of P2K1/DORN1/P2K2 in young epidermal root cells (Fig. 4e).

Cyclic Nucleotide-Gated Channel2 works together with CNGC4 in PAMP signalling, acting as a heterotrimeric $Ca^{2+}$ channel in the flagellin 22 pathway (Chin *et al.*, 2013; Tian *et al.*, 2019). During the course of this study, Wu *et al.* (2021) reported that Arabidopsis pollen grain PM has an eATP-activated $Ca^{2+}$ influx conductance, measured using whole-cell patch clamp electrophysiology. This conductance was impaired in both a single mutant of CNGC2 and a single mutant of CNGC4, suggesting that these two channel subunits might work together to facilitate germination. Whether CNGC2 and CNGC4 underpin eATP-induced $[Ca^{2+}]_{cyt}$ elevation and transcription in pollen remains untested. Here, with eATP as a potential DAMP, CNGC2 could be acting either as a homotetramer or a heterotetramer (that includes CNGC4) in the root epidermis, but in either event it is the obligate component of the depolarization response given CNGC4's redundancy (Fig. S5e–g; Table S2). If a heterotetramer included CNGC4 (which is expressed at almost half the level of CNGC2 in the epidermis; Dinneny *et al.*, 2008), that CNGC4 subunit could be replaced. This is in contrast to CNGC4's pivotal role in the PAMP signalling CNGC2/4 heterotetramer, where CNGC4 is the phosphorylation target of the BIK1 kinase (Tian *et al.*, 2019).

A residual $[Ca^{2+}]_{cyt}$ signature and a transcriptional response were still observed in CNGC2 mutants, showing that other channels are involved in the root's overall response to eATP that now need to be identified. The results here from the cortex implicate a role for CNGC4 (Figs 4e, S9f). Annexin1 is implicated at whole root level, but its mode of action is not yet determined (Mohammad-Sidik *et al.*, 2021). Extracellular ATP's upregulation of defence-related and wound-response genes *MPK3*, *WRKY40*, *CPK28*, and *MC7* is P2K1/DORN1 dependent (Choi *et al.*, 2014; Jewell *et al.*, 2019) and was significantly impaired here in *cngc2-3* (Fig. 4). Metacaspase 7 expression can be upregulated by the necrotrophic fungus *Alternaria brassicicola* (Kwon & Hwang, 2013). Its CNGC2-dependent upregulation by eATP may relate specifically to DAMP signalling following ATP release by damaged cells. Wounded root cells not only release ATP (Dark *et al.*, 2011) that could act as a DAMP for their neighbours but also release another DAMP, the peptide PLANT ELICITOR PEPTIDE 1 (PEP1; Hander *et al.*, 2019). This is perceived in neighbouring cells by the cognate PM receptors PEP1 RECEPTOR 1 (PEPR1) and PEPR2 that relay to CNGC2 to cause $[Ca^{2+}]_{cyt}$ elevation (Qi *et al.*, 2010). *PEPR2* is coexpressed with *P2K1/DORN1* (Tripathi *et al.*, 2017). Extracellular ATP also upregulates *PEPR1* and *PEPR2* transcription (Jewell *et al.*, 2019), so CNGC2 could be a common component in these DAMP pathways to facilitate the adaptive response.

## Acknowledgements

This work was funded by the UK Research and Innovation's Biotechnology and Biological Sciences Research Council (BBSRC; BB/J014540/1); the framework of the third call of the ERA-NET for Coordinating Action in Plant Sciences, with funding from the BBSRC (BB/S004637/1), the US National Science Foundation (grant no. 1826803), and the Agence Nationale de la Recherche; the University of Cambridge Commonwealth, European and International Trust; Jiangsu Normal University; and a Discovery grant from the National Science and Engineering Research Council to KY. We thank Ms S. Chakraborty and Mr A. Sharif for technical assistance and Prof. G. Berkowitz for *dnd1*.

## Author contributions

JS, BM, NL-F, VL, GS, JMD: Project conception. LW, YN, JS, REM, EM, KAW, AD, A-AV, LR, KY, WM, JMD: Experimental design, execution, and analyses. All authors contributed to writing.

## ORCID

Julia M. Davies https://orcid.org/0000-0003-2630-4339
Nathalie Leblanc-Fournier https://orcid.org/0000-0002-6079-1583
Valérie Legué https://orcid.org/0000-0003-2090-9580
Elsa Matthus https://orcid.org/0000-0002-7845-3945
Wolfgang Moeder https://orcid.org/0000-0003-3889-6183
Bruno Moulia https://orcid.org/0000-0002-3099-0207
Lourdes Rubio https://orcid.org/0000-0002-7747-2722
Gary Stacey https://orcid.org/0000-0001-5914-2247
Jian Sun https://orcid.org/0000-0002-1434-4029
Anne-Aliénor Véry https://orcid.org/0000-0003-1961-5243
Limin Wang https://orcid.org/0000-0003-2018-3441
Katie A. Wilkins https://orcid.org/0000-0001-6513-856X
Keiko Yoshioka https://orcid.org/0000-0002-3797-4277

## Data availability

All lines and data will be made available in a timely manner upon request.



© 2022 The Authors
*New Phytologist* © 2022 New Phytologist Foundation

## References

**Al-Younis I, Moosa B, Kwiatkowski M, Jaworski K, Wong A, Gehring C. 2021**. Functional crypto-adenylate cyclases operate in complex plant proteins. *Frontiers in Plant Science* **12**: e711749.

**Chakraborty S, Toyota M, Moeder W, Chin K, Fortuna A, Champigny M, Vanneste S, Gilroy S, Beeckman T, Nambara E *et al.* 2021**. Cyclic Nucleotide-Gated Ion Channel 2 modulates auxin homeostasis and signaling. *Plant Physiology* **187**: 1690–1703.

**Chin K, DeFalco TA, Moeder W, Yoshioka K. 2013**. The *Arabidopsis* cyclic nucleotide-gated ion channels AtCNGC2 and AtCNGC4 work in the same signaling pathway to regulate pathogen defense and floral transition. *Plant Physiology* **163**: 611–624.

**Choi J, Tanaka K, Cao Y, Qi Y, Qiu J, Liang Y, Lee SY, Stacey G. 2014**. Identification of a plant receptor for extracellular ATP. *Science* **343**: 290–294.

**Dark** A, **Demidchik** V, **Richards** SL, **Shabala** S, **Davies** JM. 2011. Release of extracellular purines from plant roots and effect on ion fluxes. *Plant Signaling and Behavior* **6**: 1855–1857.

**Demidchik V, Bowen HC, Maathuis FJM, Shabala SN, Tester MA, White PJ, Davies JM. 2002**. *Arabidopsis thaliana* root non-selective cation channels mediate calcium uptake and are involved in growth. *The Plant Journal* **32**: 799–808.

**Demidchik V, Nichols C, Dark A, Oliynyk M, Glover BJ, Davies JM. 2003**. Is ATP a signaling agent in plants? *Plant Physiology* **133**: 456–461.

**Demidchik V, Shang Z, Shin R, Thompson E, Rubio L, Laohavisit A, Mortimer JC, Chivasa S, Slabas AR, Glover BJ. 2009**. Plant extracellular ATP signalling by plasma membrane NADPH oxidase and $Ca^{2+}$ channels. *The Plant Journal* **58**: 903–913.

**Dindas J, Scherzer S, Roelfsema MRG, von Meyer K, Müller HM, Al-Rasheid KAS, Palme K, Dietrich P, Becker D, Bennett MJ *et al.* 2018**. AUX1-mediated root hair auxin influx governs $SCF^{TIR1/AFB}$-type $Ca^{2+}$ signaling. *Nature Communications* **9**: e1174.

**Dinneny JR, Long TA, Wang JY, Jung JW, Mace D, Pointer S, Barron C, Brady SM, Schiefelbein J, Benfey PN. 2008**. Cell identity mediates the response of *Arabidopsis* roots to abiotic stress. *Science* **320**: 942–945.

**Hander T, Fernández-Fernández Á D, Kumpf RP, Willems P, Schatowitz H, Rombaut D, Staes A, Nolf J, Pottie R, Yao P *et al.* 2019** Damage on plants activates $Ca^{2+}$ -dependent metacaspases for release of immunomodulatory peptides. *Science*, **363**: 1301–1311.

**Jaffe M. 1973**. The role of ATP in mechanically stimulated rapid closure of the Venus's flytrap. *Plant Physiology* **51**: 17–18.

**Jarratt-Barnham E, Wang L, Ning Y, Davies JM. 2021**. The complex story of plant cyclic nucleotide-gated channels. *International Journal of Molecular Sciences* **22**: 874.

**Jewell JB, Sowders JM, He R, Willis MA, Gang DR, Tanaka K. 2019**. Extracellular ATP shapes a defense-related transcriptome both independently and along with other defense signaling pathways. *Plant Physiology* **179**: 1144–1158.

**Knight H, Trewavas AJ, Knight MR. 1997**. Recombinant aequorin methods for measurement of intracellular calcium in plants. In: Gelvin SB, Schilperoort RA, eds. *Plant molecular biology manual*. Dordrecht, the Netherlands: Springer, 1–22.

**Krogman W, Sparks JA, Blancaflor EB. 2020**. Cell type-specific imaging of calcium signaling in *Arabidopsis thaliana* seedling roots using GCaMP3. *International Journal of Molecular Sciences* **21**: 6385–6399.

**Kumar S, Tripathi D, Okubara PA, Tanaka K. 2020**. Purinoceptor P2K1/DORN1 enhances plant resistance against a soilborne fungal pathogen, *Rhizoctonia solani*. *Frontiers in Plant Science* **11**: e1479.

**Kwon SI, Hwang DJ. 2013**. Expression analysis of the metacaspase gene family in *Arabidopsis*. *Journal of Plant Biology* **56**: 391–398.

**Lew RR, Dearnaley JD. 2000**. Extracellular nucleotide effects on the electrical properties of growing *Arabidopsis thaliana* root hairs. *Plant Science* **153**: 1–6.

**Matthus E, Sun J, Wang L, Bhat MG, Mohammad-Sidik AB, Wilkins KA, Leblanc-Fournier N, Legué V, Moulia B, Stacey G *et al.* 2019a**. DORN1/P2K1 and purino-calcium signalling in plants: making waves with extracellular ATP. *Annals of Botany* **124**: 1227–1242.

**Matthus E, Wilkins KA, Swarbreck SM, Doddrell NH, Doccula FG, Costa A, Davies JM. 2019b**. Phosphate starvation alters abiotic-stress-induced cytosolic free calcium increases in roots. *Plant Physiology* **179**: 1754–1767.

**Mohammad-Sidik A, Sun J, Shin R, Song Z, Ning Y, Matthus E, Wilkins KA, Davies JM. 2021**. *Annexin 1* is a component of eATP-induced cytosolic calcium elevation in *Arabidopsis thaliana* roots. *International Journal of Molecular Sciences* **22**: 494.

**Pham AQ, Cho S-H, Nguyen CT, Stacey G. 2020**. *Arabidopsis* lectin receptor kinase P2K2 is a second plant receptor for extracellular ATP and contributes to innate immunity. *Plant Physiology* **183**: 1364–1375.

**Qi Z, Verma R, Gehring C, Yamaguchi Y, Zhao Y, Ryan CA, Berkowitz GA. 2010**. $Ca^{2+}$ signaling by plant *Arabidopsis thaliana* Pep peptides depends on AtPepR1, a receptor with guanylyl cyclase activity, and cGMP-activated $Ca^{2+}$ channels. *Proceedings of the National Academy of Sciences, USA* **107**: 21193–21198.

**Rincón-Zachary M, Teaster ND, Sparks JA, Valster AH, Motes CM, Blancaflor EB. 2010**. Fluorescence resonance energy transfer-sensitized emission of yellow cameleon 3.60 reveals root zone-specific calcium signatures in *Arabidopsis* in response to aluminum and other trivalent cations. *Plant Physiology* **152**: 1442–1458.

**Tanaka K, Swanson SJ, Gilroy S, Stacey G. 2010**. Extracellular nucleotides elicit cytosolic free calcium oscillations in *Arabidopsis*. *Plant Physiology* **154**: 705–719.

**Tian W, Hou C, Ren Z, Wang C, Zhao F, Dahlbeck D, Hu S, Zhang L, Niu Q, Li L *et al.* 2019**. A calmodulin-gated calcium channel links pathogen patterns to plant immunity. *Nature* **572**: 131–135.

**Tripathi D, Zhang T, Koo AJ, Stacey G, Tanaka K. 2017**. Extracellular ATP acts on jasmonate signaling to reinforce plant defense. *Plant Physiology* **176**: 511–523.

**Waadt R, Köster P, Andrés Z, Waadt C, Bradamante G, Lampou K, Kudla J, Schumacher K. 2020**. Dual-reporting transcriptionally linked genetically encoded fluorescent indicators resolve the spatiotemporal coordination of cytosolic abscisic acid and second messenger dynamics in *Arabidopsis*. *Plant Cell* **32**: 2582–2601.

**Wang L, Stacey G, Leblanc-Fournier N, Legué V, Moulia B, Davies JM. 2019**. Early extracellular ATP signaling in *Arabidopsis* root epidermis: a multi-conductance process. *Frontiers in Plant Science* **10**: e1064.

**Wang L, Wikins K, Davies J. 2018**. *Arabidopsis* DORN1 extracellular ATP receptor; activation of plasma membrane $K^+$ and $Ca^{2+}$-permeable conductances. *New Phytologist* **218**: 1301–1304.

**Wang Y-F, Munemasa S, Nishimura N, Ren H-M, Robert N, Han M, Puzõrjova I, Kollist H, Lee S, Mori I. 2013**. Identification of cyclic GMP-activated nonselective $Ca^{2+}$-permeable cation channels and associated *CNGC5* and *CNGC6* genes in *Arabidopsis* guard cells. *Plant Physiology* **163**: 578–590.

**Wu Y, Yin H, Liu X, Xu J, Qin B, Feng K, Kang E, Shang Z. 2021**. P2K1 receptor, heterotrimeric Gα protein and CNGC2/4 are involved in extracellular ATP-promoted ion influx in the pollen of *Arabidopsis thaliana*. *Plants* **10**: e1743.

## Supporting Information

Additional Supporting Information may be found online in the Supporting Information section at the end of the article.

**Fig. S1** Controls for depolarization of elongation zone epidermis and effect of extracellular $Ca^{2+}$ chelation or channel block.

**Fig. S2** Growth of *cngc2-3* and receptor expression.

**Fig. S3** Extracellular ATP (eATP) did not depolarize *dnd1* elongation zone epidermis.

**Fig. S4** Single receptor mutants supported a small but significant extracellular ATP (eATP)-induced depolarization of elongation zone epidermal $E_m$.

**Fig. S5** The *p2k1p2k2* double receptor mutant lacked the extracellular ATP (eATP)-induced depolarization of elongation zone epidermal $E_m$.

© 2022 The Authors
*New Phytologist* © 2022 New Phytologist Foundation

**Fig. S6** *cngc4-5* supported a significant extracellular ATP (eATP)-induced depolarization of elongation zone epidermal $E_m$.

**Fig. S7** Extracellular ATP (eATP) did not activate inward currents in *dorn1-3* root elongation zone epidermal protoplasts.

**Fig. S8** Cyclic Nucleotide-Gated Channel2 (CNGC2) contributed to the extracellular ATP (eATP)-induced $[Ca^{2+}]_{cyt}$ increase in roots.

**Fig. S9** Cyclic Nucleotide-Gated Channel2 (CNGC2) is not required for extracellular ATP (eATP)-induced depolarization of primary root elongation zone cortical plasma membrane potential but CNGC4 is involved.

**Methods S1** Genotyping *cngc* insertional and complemented mutants.

**Methods S2** Growth conditions.

**Methods S3** Membrane voltage measurement.

**Methods S4** Patch clamp recordings.

**Methods S5** Quantitative real-time PCR analysis of gene expression.

**Table S1** Primers used for genotyping transfer DNA mutant lines and quantitative real-time PCR.

**Table S2** Mean ± SE membrane voltage $E_m$ measurements.

Please note: Wiley Blackwell are not responsible for the content or functionality of any Supporting Information supplied by the authors. Any queries (other than missing material) should be directed to the *New Phytologist* Central Office.



© 2022 The Authors
*New Phytologist* © 2022 New Phytologist Foundation